DOI: https://doi.org/10.1103/PhysRevB.111.054112
https://journals.aps.org/prb/abstract/10.1103/PhysRevB.111.054112
Submitted 10 October 2024

Oxygen vacancies in semiconducting $BaTiO_3$ based ferroelectrics: electron doping, history dependence of T_C and domain wall pinning

Francesco Cordero,[1,*] Floriana Craciun,[1] Paulo Sergio da Silva, Jr.,[2]
Michel Venet Zambrano,[2] Elisa Mercadelli,[3,†] and Pietro Galizia[3]

[1]*Istituto di Struttura della Materia-CNR (ISM-CNR), Area della Ricerca di Roma - Tor Vergata, Via del Fosso del Cavaliere 100, I-00133 Roma, Italy*
[2]*Department of Physics, Federal University of São Carlos, 13565-905 São Carlos, Brazil*
[3]*Institute of Science, Technology and Sustainability for Ceramics - CNR (ISSMC-CNR), Via Granarolo 64, 48018 Faenza, Italy*

(Dated: February 1, 2025)

We measured the complex Young's modulus of $BaTiO_{3-\delta}$, (BT) $Ba_xSr_{1-x}TiO_{3-\delta}$ (BST) and $(Ba_{0.85}Ca_{0.15})(Zr_{0.1}Ti_{0.9})O_{3-\delta}$ (BCTZ) during heating and cooling runs at various O deficiencies (which dope electrons rendering the samples semiconducting/conducting ferroelectrics) and aging times. The elastic energy loss has peaks due to the jumps of isolated O vacancies (V_O) and reorientations of pairs of V_O in the paraelectric phase, from which the respective rates and activation energies are measured. These rates control the mechanisms of domain clamping, pinning, fatigue, and anything related to the V_O mobility. In the ferroelectric (FE) phase, the drop of the losses due to the domain wall motion upon introduction of V_O monitors the degree of pinning. In addition, large shifts of T_C are observed at the same value of δ upon varying the permanence time in the FE state, up to $\Delta T_C = 21$ K in BST, while no aging effect is found in BCTZ.

The phenomenology is explained by considering that T_C is depressed mainly by the mobile electrons doped by V_O. Each isolated V_O dopes two electrons as itinerant Ti^{3+} ions, but, when it forms a stable linear V_O–Ti^{2+}–V_O pair, the two electrons of the Ti^{2+} are subtracted from the mobile ones, halving doping. The rise of T_C during the initial aging is then explained in terms of the progressive aggregation of the V_O. Prolonging aging for years leads to a decrease of T_C, explained assuming that the most stable position of a V_O is at 90° domain walls, whose geometry is incompatible with the pairs. Then, after enough time the V_O initially aggregated within the domains dissociate to decorate the 90° walls, increasing doping and lowering T_C.

The absence of such effects in BCTZ is due to larger activation energy for pair reorientation and pair binding energy. Then, at room temperature practically all V_O are paired and static over a time scale of hundreds of years, explaining the superior resistance of BCTZ to fatigue.

I. INTRODUCTION

The contribution of O vacancies (V_O) to fatigue and in general to the degradation of the properties of perovskite ferroelectrics has been studying since many decades[1] and is far from being fully understood. Recently it has even been proposed that many observations generally ascribed to mobile V_O on the basis of a rather loose estimation of V_O hopping barrier of ~ 1 eV, are rather due to electronic mechanisms,[2] especially after observing that the activation energy for the mean time to failure of multilayer ceramic capacitors is ~ 1.6 eV, close to a half the energy band gap of $BaTiO_3$[3]. Yet, it is undeniable that V_O are present, especially in devices, such as multi layer ceramic capacitors (MLCCs), having electrodes made of oxidizable non noble metals. Such electrodes require that the ceramics are sintered in reducing atmosphere, with a subsequent mild oxygenation, which does not fully eliminate the V_O[4,5]. Whatever the origin of the mobile charges, whether associated with V_O or other defects, an increase of the electrical conductivity is generally detrimental to applications based on insulating ferroelectrics.

On the other hand, V_O are not only detrimental to the materials properties, since the traditional method for hardening the piezoelectrics, namely reducing their losses, through domain wall (DW) pinning is to introduce V_O by acceptor doping[1]. Another possible effect of introducing acceptor-V_O pairs is enhancing the electrostrain in piezoceramics, though the exact mechanisms involved are not yet clear[6], but all these effect are greatly affected by rises in temperature, due the increased mobility of V_O[7].

It is therefore important to improve our knowledge of the behavior of V_O in ferroelectric materials at the atomic scale: their mobility, how they aggregate, and are trapped by dopants and DWs. This is usually done with methods that probe the long range diffusion, such as measuring the change of mass or resistivity of samples during annealing in controlled atmospheres, or the isotope tracer diffusion technique[4,8,9]. These methods, however, reveal the overall diffusion and not the different steps involved, especially when carried out at high temperatures, where the aggregation of V_O into pairs and chains[10,11] becomes irrelevant.

Indeed, selectively probing the different types of jumps of V_O and measuring their concentration is not easy. An isolated V_O has an anisotropic elastic dipole but no electric dipole; therefore its hopping cannot be probed by dielectric but only by anelastic spectroscopy, unless it is associated with another charged point defect, *e.g.* cation vacancy, to form an electric dipole. Also NMR relaxation can selectively probe the different types of jumps of V_O, but it has been used only few times[12,13], while EPR has been used only for studying the kinetics of V_O trapped by acceptors[14]. As a consequence, the link between the V_O mobility and fatigue or degradation phenomena in ferroelectric perovskites is generally vague, without determining a detailed microscopic mechanism. Certainly the ionic contribution of V_O to conductivity is negligible compared to the polaronic and electronic ones[15], but their hopping

as reorienting elastic dipoles, as electric dipoles when paired with a charged defect, and their migration to domain walls differently affect the ferroelectric properties at room temperature over time scales from minutes to months or years, even in the absence of electric excitation.

Here we present a study of the mobility and clustering of V_O introduced by reducing treatments in $BaTiO_3$ (BT), $Ba_xSr_{1-x}TiO_3$ (BST) and $(Ba_{0.85}Ca_{0.15})(Zr_{0.1}Ti_{0.9})O_3$ (BCTZ), which are found to have very different hopping rates, depending on their aggregation state and material composition, and introduce history dependent effects on the Curie temperature T_C. Novel microscopic insight is provided on how V_O contribute to electron doping and pinning of domain walls, finally leading to aging and fatigue. In particular, it is shown how the electron doping is strongly affected by the degree of clustering of the V_O.

The Discussion is organized as follows: Sect. A is an overview of the interpretation of the anelastic spectra, based on previous work on $SrTiO_3$ and $BaTiO_3$, and includes a simplified analysis of the new spectra of BCTZ. In addition to the peaks due to the various types of jumps of the V_O, also their pinning of domain walls is discussed, because it will be involved in the long term aging effects on T_C. In Sect. B the known mechanisms of enhancement of T_C from mobile defects are shown to be inadequate to explain the presently observed large shifts. In Sect. C it is described how the distribution and hopping of V_O should be affected by the formation of tetragonal ferroelectric domains. Until now there is no experimental evidence but only first-principle calculations on this type of information. Section D explains how the pairing and clustering of the V_O reduces the doping of mobile electrons, resulting in the major cause of change of T_C upon history. The initial rise of T_C with the aging time is explained with the slow kinetics for V_O aggregation within the ferroelectric domains. Section E deals with the final decrease of T_C on a longer time scale, which would result from the fact that an V_O has lower energy when isolated at a 90° domain wall than paired within a domain, and it takes a longer time for the paired V_O to reach the 90° DWs.

Differently from the normal conditions found in applications, namely insulating dielectrics with electric fields applied via electrodes, the materials studied here, with $0.3\% - 1.5\%$ of uncompensated V_O, are conductive and with a dark color and are studied without application of electrodes and electric fields. Nonetheless, the microscopic mechanisms of V_O hopping, clustering, pinning and migration to domain walls discussed here always occur, whether in the usual insulating conditions or in locally highly doped degraded states, unless the local concentration is so high to induce ordered O deficient phases[16]. The doping conditions of our samples may be representative of the initial stages of such type of degradation.

II. EXPERIMENTAL

Two $BaTiO_3$ samples BT1 and BT2 were cut from a bar prepared by conventional mixed-oxide powder technique at the Department of Chemistry of the Martin Luther University Halle (Saale), Germany, as described in[17]. The present sample BT1, with dimensions $43 \times 4.1 \times 0.59$ mm^3, corresponds to bar No. 2 in that paper, while the present sample BT2 is a bar $43 \times 4.1 \times 1.1$ mm^3. Sample BT3 was another bar $32.9 \times 4.2 \times 1.15$ mm^3 of $BaTiO_3$ prepared in the same laboratory. Sample BT4, $42 \times 6.3 \times 0.67$ mm^3, was prepared, again by conventional mixed-oxide powder technique, at the Physics Department of UFSCar, São Carlos (Brazil), as described in[17], and corresponds to sample No. 1.1 of that paper and sample BT #1 in[18].

The BST samples were prepared in UFSCar, as described in[19]. The bar with $x = 0.03$ had dimensions $34.4 \times 4.4 \times 0.43$ mm^3.

The $(Ba_{0.85}Ca_{0.15})(Zr_{0.1}Ti_{0.9})O_3$ was synthesized via the solid-state reaction method using $BaCO_3$ (Aldrich, $> 99\%$ purity), $CaCO_3$ (MERCK, $> 99\%$ purity), TiO_2 (Degussa P25, $> 99.5\%$ purity), and ZrO_2 (MEL, SC 101, $> 99\%$ purity) as starting materials. The oxide powders were mixed and ball–milled for 20 hours, then pressed and calcined at 1300 °C for 5 hours. The calcined powders were further ball–milled for 96 hours and sieved to 200 μm. Green bars were formed by uniaxial pressing at 100 MPa, followed by cold isostatic pressing at 300 MPa. Sintering was performed in a covered ZrO_2 box with samples embedded in BCTZ-50 powders, at 1500 °C for 4 hours, with natural cooling in the furnace. Two bars were cut to $47.9 \times 5.5 \times 0.57$ mm^3 (BCTZ1) and $33 \times 5.5 \times 0.55$ mm^3 (BCTZ2).

Oxygen vacancies were introduced by exposing the bars to a flow of 0.1CO + 0.9Ar at 1 bar and high temperature ($970 - 1250$ °C) for up to 2 h, followed by 1 h homogenization at 800 °C in the same reducing flow and cooling to room temperature (RT) in few minutes. The sample was first wrapped in a Pt foil with open ends, using slabs of Al_2O_3 or Y-stabilized ZrO_2 to avoid the contact with Pt. The Pt envelope was placed in a quartz tube with water cooled jacket and heated by induction. Its temperature was measured with a pyrometer Land M1 600/100C-S and a hot-wire pyrometer Pirottico SAE, insensitive to changes in emissivity. The reduced samples become dark and conducting, due to the doped mobile electrons, a condition that is quite different from conventional insulating ferroelectrics, but that might approximate the damaged regions near the electrodes in degraded devices[16,20]. The concentration of V_O was estimated from the mass reduction after the treatment, and might be overestimated by unwanted loss of BaO, especially at the highest temperatures. In fact, while the total mass loss of BT1 after all the treatments corresponded to $\delta = 0.0118$, the mass gain after reoxygenation corresponded to $-\delta = 0.00763$, but the sample was again pale yellow with no trace of V_O in the anelastic spectrum. Furthermore, the anelastic spectra of the as-prepared and reoxidized sample were almost identical (Fig. 2), indicating that the effects of the possible introduction of Ba vacancies or other defects during the heat treatments were irrelevant. Sample BT2 was subjected to the reductions together with BT1 for control, without measuring its anelastic spectrum. Its state with $\delta = 0.00935$ corresponds to the final $\delta = 0.0118$ of BT1, and the fact that δ estimated from the total mass losses is smaller in the thicker sample is in agreement with the hypothesis of

an overestimation of δ from unwanted losses of BaO.

The complex Young's modulus $E = E' + iE''$ was measured by suspending the sample with two thin thermocouple wires in vacuum and electrostatically exciting its free-free flexural resonances, as described in[21]. In order to short the thermocouple wires, one of which grounded, and make the sample conductive in correspondence with the exciting/measuring electrode, silver paint was applied to the sample. The Young's modulus is measured from the resonance frequency[22]

$$f = 1.028 \frac{h}{l^2} \sqrt{\frac{E}{\rho}}\,, \qquad (1)$$

where l, h, and ρ are the sample's length, thickness, and density, assumed as constants, since they vary much less than E with temperature. The elastic energy loss, $Q^{-1} = E''/E'$, was measured from the decay of the free oscillations, after switching off the excitation, or from the width of the resonance curves. The frequency dependence of the anelastic spectra was measured by exciting up to three flexural modes, with frequencies in the ratios $1 : 5.4 : 13$, during the same run. The anelastic relaxation from the hopping of a V_O, and consequent reorientation of its elastic dipole, causes a Debye peak in the energy loss measured at frequency $\omega/2\pi$, with maximum at the temperature such that $\omega\tau \simeq 1$, where τ is close to the mean hopping time[22].

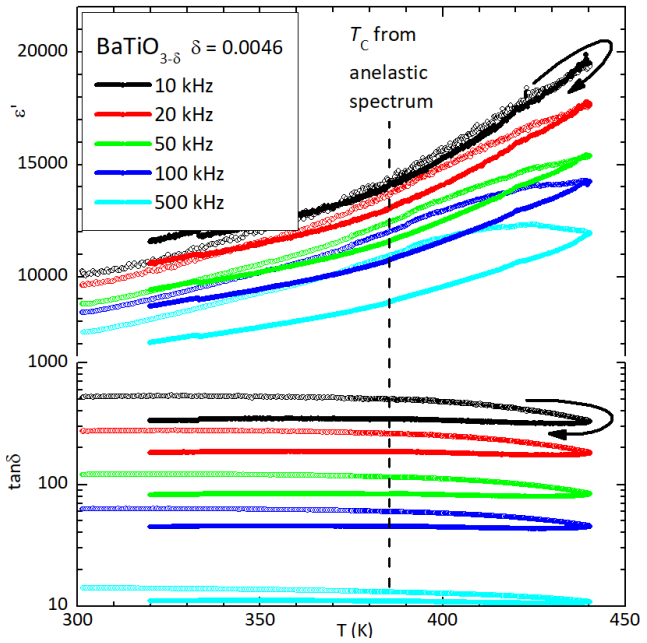

FIG. 1: Dielectric spectrum of $BaTiO_{3-\delta}$, $\delta = 0.0046$, with $T_C = 385$ K, deduced by the anelastic spectrum (not shown).

We did not pursue a parallel dielectric characterization of the samples, since the dielectric spectra do not provide any direct information on isolated or aggregated V_O, which lack electric dipoles, unless associated with acceptor impurities. Moreover, the dielectric losses due to the electronic conduction were so high in the reduced samples, that it was impossible to distinguish T_C. As an example, Fig. 1 shows the dielectric spectrum measured on a $BaTiO_{3-\delta}$ sample with $\delta = 0.0046$ and $T_C = 385$ K, deduced from the anelastic spectrum.

III. RESULTS

A. $BaTiO_{3-\delta}$

Figure 2 presents the anelastic spectra of sample BT1 of $BaTiO_{3-\delta}$ at increasing O deficiencies δ. The curves are perfectly similar to those measured in BT4 and already published[18]. The introduction of V_O has three major effects: *i)* shift T_C to lower temperature, *ii)* introduce thermally activated anelastic relaxation peaks in the paraelectric phase, *iii)* substantially reduce the elastic energy loss from the relaxational motion of DWs in the tetragonal ferroelectric phase. Peak P_F, only visible when T_C is lowered enough, is due to the hopping of isolated (free) V_O, while peak P_P is due to the reorientation of V_O pairs[18]. At higher temperature, two minor peaks are found, which grow with δ much less than P_F and P_P, and are attributed to V_O trapped by native defects, such as Ba vacancies[18].

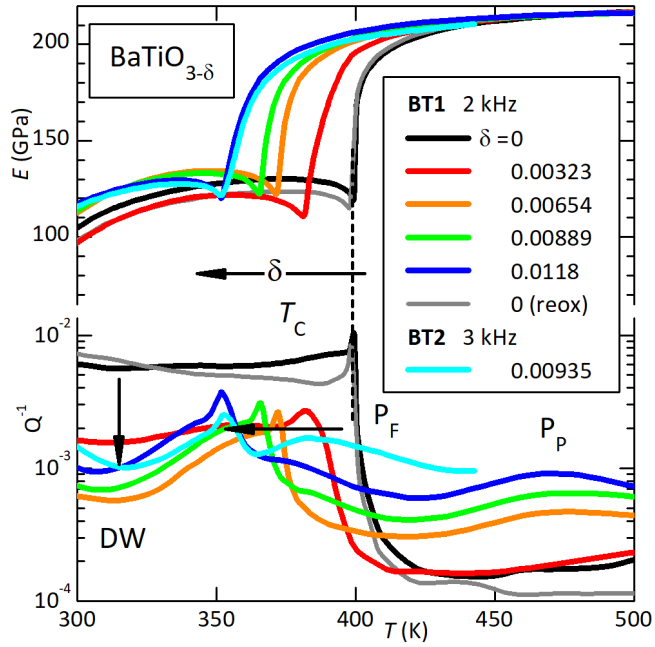

FIG. 2: Young's modulus E and elastic energy loss Q^{-1} of the two samples BT1 and BT2 cut from the same bar of $BaTiO_3$ at various O deficiencies δ.

All these curves are measured during cooling within few days after the reduction treatment or after a temperature run extending at least to 500 K, therefore after few days in the FE

state. The last curve of BT1 (thin gray) was obtained after re-oxygenating the sample in air at 1100 °C for 90 min. It is very similar to the initial black curve, and has a high–temperature background even lower, indicating that no major degradation occurred during the previous reductions.

The anelastic measurements on BT2, which had been always reduced together with BT1, started 6 years after the last reduction and the curve in Fig. 2 was measured during the fourth cooling cycle. It is very close to the blue curve of BT1, supposedly in a similar state, except for a higher intensity of peak P_F.

Figure 3 presents various $E(T)$ curves of $BaTiO_{3-\delta}$ around T_C measured under different conditions. Apart from differences in the precursor softening above T_C, which may also be affected by an additional transition above T_C (see beginning of Discussion), the interest is in the fact that T_C, at the lower edge of the curves, may vary considerably in the same sample at constant O deficiency. As expected, T_C is stable in the absence of V_O (Fig. 3a), but it depends on how long the sample aged in the ferroelectric phase when measured during heating in O deficient samples, already with δ as low as 0.003. In Figs. 3b,c there is an increase of T_C with increasing the aging time at RT in the range of hours and days, with the highest T_C achieved after a night at liquid N_2 temperature (LNT).

Figure 4a, however, shows that T_C does not increase indefinitely and saturate with aging, since the lowest value of T_C during heating is measured after aging 6 years, with a huge inverse thermal hysteresis of 10 K (curves 1 and 2). Then T_C remains stable with normal hysteresis, if cycling does not exceed 600 K (curves 3-8, only two of which are shown for clarity), but, after reaching 800 K, it increases of 5 K and remains stable there (curves 20-24). Figure 4b shows the Q^{-1} curves corresponding to 1 and 2 in Fig. 4a, after 6 years aging. Peak P_F during cooling is shifted to higher temperature, together with T_C, and has smaller intensity.

B. $Ba_xSr_{1-x}TiO_3$

Substitution of 3% Ba with Sr decreases T_C of $BaTiO_3$ from 400 K to 390 K, independent of history (Fig. 5a); yet, upon introduction of V_O the temperature span of the changes of T_C is increased with respect to $BaTiO_{3-\delta}$. Such a span, only for heating, is ~ 6 K in $BaTiO_{3-\delta}$ with $\delta \simeq 0.003$ and 0.009, but is 21 K in $Ba_{0.97}Sr_{0.03}TiO_{3-\delta}$ with $\delta \simeq 0.005$ (Fig. 5b).

Again, there is a trend of higher T_C for longer permanence at RT in the range of hours and few days, but 14 days aging lowers T_C, reminding the long aging effect in Fig. 4a. Few data are available for $x(\mathrm{Sr}) = 0.1$, but a shift of 7 K in T_C has been observed also there (Fig. 5c).

C. $(Ba_{0.85}Ca_{0.15})(Zr_{0.1}Ti_{0.9})O_3$

Figure 6 presents the anelastic spectra of BCTZ at various O deficiencies, measured during both heating and cooling. The three phase transitions of $BaTiO_3$ from the cubic paraelectric phase to the tetragonal, orthorhombic and rhombohedral ferroelectric phases are clearly recognizable in the as prepared oxygenated state. The introduction of V_O shifts to lower temperature T_C and T_{OT}, which are still separated at $\delta \simeq 0.005$, but beyond that value the elastic anomalies merge into a broad one.

Also the anelastic relaxation peaks in the paraelectric phase, due to isolated (P_F) and paired (P_P) V_O are recognizable, but there are two major differences with respect to $BaTiO_{3-\delta}$ (Fig. 2): the two peaks are shifted to higher temperature and are much broader.

In order to be more quantitative, we fitted the anelastic spectrum of BCTZ above T_C, following the example of $BaTiO_3$[18], with the phenomenological expressions[22,23]

$$Q^{-1} = \frac{\Delta}{T\cosh^2(A/2k_BT)}\frac{1}{(\omega\overline{\tau})^{\alpha}+(\omega\overline{\tau})^{-\beta}} \quad (2)$$

$$\overline{\tau} = \tau_0 \exp(W/k_BT)/\cosh(A/2k_BT) \quad (3)$$

where the usual Debye peak, when $\alpha = \beta = 1$, and Arrhenius law for the relaxation time over a barrier W are modified in order to describe relaxation between initial and final states differing in energy by A, due to non–equivalence of initial and final state or disorder; this accounts for intensities of the peaks that do not decrease as $1/T$ with increasing T. In view of the asymmetric shape of peak P_P, two broadening parameters have been introduced for the low–temperature (α) and high–temperature (β) sides of the peaks. The high quality anelastic spectra of $SrTiO_{3-\delta}$ had been fitted with three distinct peaks, including the intermediate relaxation P_I from the asymmetric jumps of formation/dissociation of the pairs[10], and those of $BaTiO_{3-\delta}$ with up to five peaks, when distinct peaks appeared at higher temperatures, attributed to V_O trapped by unwanted defects[18]. In $(Ba_{0.85}Ca_{0.15})(Zr_{0.1}Ti_{0.9})O_3$ the lattice disorder broadens the relaxation spectrum so much that it is impossible to distinguish more than two peaks, and therefore the fits were carried out with two peaks, Eq. (2), plus a linear background and an exponential, $A\exp(B/T)$, to take into account the rise of dissipation on approaching T_C.

Fits to the anelastic spectra of the lowest and highest O deficiencies are presented in Fig. 7, while the fitting parameters are reported in Table I, together with those of two spectra of $BaTiO_{3-\delta}$ from Ref.[18].

Finally, Fig. 8 shows that, while the slight lattice disorder of 3% Sr substituting Ba amplifies the dependence of T_C on aging (Fig. 5 compared with Fig. 3), the strong lattice disorder in BCTZ depresses it. The three heating curves differ only in degree of softening, but have the same $T_C \simeq 315$ K.

TABLE I: Fitting parameters of the anelastic spectra of BT (from Ref.[18]) and BCTZ in Fig. 7.

	BT	BT	BCTZ	BCTZ
δ	0.0027	0.0153	0.00419	0.0108
P_F: W_F (eV)		0.72	0.734	0.804
τ_0 (s)		2.6×10^{-14}	1×10^{-13}	2.6×10^{-14}
$\alpha=\beta$		0.84	0.2	0.2
τ(293 K)		70 ms	0.4 s	2 s
P_P: W_P (eV)	0.86	0.85	1.39	1.39
τ_0 (s)	9×10^{-14}	4.7×10^{-14}	5.3×10^{-15}	8.6×10^{-15}
α	0.91	0.80	0.38	0.24
β	0.91	0.80	0.53	1
τ(293 K)	60 s	20 s	130 y	200 y

IV. DISCUSSION

The above results show that the V_O not only decrease T_C, but also make it strongly dependent on history in BT and BST up to 10% Sr but not in BCTZ. It should be mentioned that the V_O also introduce a new phase transition in $BaTiO_{3-\delta}$ slightly above T_C, which is hardly visible in the anelastic spectra measured at lower frequency shown here, but is apparent in the modulus measured at higher frequency. It might be a local effect of stabilization of the ferroelectric phase around particular clusters of V_O, and it will be the object of a separate study. The additional transition does not invalidate the fact that there is a major FE transition at a T_C that depends on both δ and history. We will try to explain these observations in terms of the most obvious mechanisms that are possible when V_O are the only or major defect species: pairing and clustering of V_O and their association with domain walls.

The reduced samples, with $0.3\% - 1.5\%$ uncompensated V_O, are conductive and with a dark color, differently from the ideal insulating conditions required in applications, but similarly to the defective regions, usually near non-noble metal electrodes, of degraded capacitors and devices. Indeed, it is known since a long time that, at the Ni electrodes of multilayer ceramic capacitors, the concentration of V_O may be so high that they form ordered defect structures[16], and concentrations of V_O as high as 6% have been measured by XPS[20]. The microscopic mechanisms of V_O hopping, clustering, pinning and migration to domain walls discussed here are valid in the conducting and insulating conditions, at least until their concentration is within the range tested here. An influence of electron doping is found on the V_O hopping barriers, which are gradually depressed with increase of O deficiency and hence doping.

A. General interpretation of the anelastic spectra

1. *Hopping of isolated and paired O vacancies*

We refer to previous articles for the detailed analysis and discussion of the anelastic spectra of $SrTiO_{3-\delta}$[10] and $BaTiO_{3-\delta}$[18], just reminding that the hopping of an V_O reorients the associated elastic dipole with major axis parallel to the nearest neighbor Ti atoms, causing peaks of the form Eq. (2). The hopping of isolated V_O causes peak P_F, from which the hopping barrier in $SrTiO_3$ is evaluated as $W_F = 0.60$ eV, independent of δ, and in $BaTiO_{3-\delta}$ is ~ 0.73 eV and decreases with doping. Peak P_P arises from the reorientation of V_O pairs and has a higher activation energy, $W_P = 1.0$ eV in $SrTiO_{3-\delta}$, 0.86 eV in $BaTiO_{3-\delta}$, the latter again decreasing with doping. The lowering of the hopping barriers with doping is evident from the general shift to lower temperature of the whole anelastic spectrum of $BaTiO_{3-\delta}$ with increasing δ (Fig. 2). The activation energy for pair reorientation includes a partial dissociation of the pair and an increase of the saddle point energy corresponding to the electrostatic repulsion between the two approaching charged V_O. This effect has been estimated in $SrTiO_3$ as a rise of the saddle point energy for forming a pair by $\Delta W_{el} = 0.19$ eV with respect to free hopping[10], as shown in Fig. 9. It causes a slowing of the kinetics for reaching thermal equilibrium between free and aggregated V_O, with respect to what expected from the high mobility of the isolated V_O. A similar effect had been recognized to play a role with the highly mobile O atoms of the CuO_x planes in $YBa_2Cu_3O_{6+x}$[24].

The actual shape of the potential of the intermediate step 4 for the pair reorientation (Fig. 9) is not easy to probe with anelasticity, since the corresponding peak P_I is depressed by the asymmetry factor in Eq. (2). In $SrTiO_{3-\delta}$, with its nearly pure Debye peaks, it can be distinguished in ceramic samples[25], but hardly in $\langle 100\rangle$ crystals[10], due to symmetry reasons. Yet, both the site and saddle point energies of configuration 4 should be intermediate between those of 2 and 3. This means that the highest barrier for the complete reorientation process between 3 and 5, probed by peak P_P, is smaller than that for dissociation from 3 to 2, and *the dissociation rate is slower than indicated by peak P_P*.

The lowering of the hopping barriers at higher O deficiency, observed in $BaTiO_3$ but not in $SrTiO_3$, can be explained in terms of a stronger interaction between the V_O and the nearest neighbor Ti atoms, when they are off–center[18]. Indeed, the elastic dipole of an isolated V_O is three times larger in $BaTiO_3$ than in $SrTiO_3$ and the hopping barrier is 0.73 eV against 0.60 eV. The mobile electrons doped by the V_O would

smear out the eight minima potential of the Ti atoms, reducing the effect, and making the V_O environment more similar to that of $SrTiO_3$, with a shallower potential[18]. The doping dependence of the hopping barriers, together with the facts that the anelastic relaxation peaks of $BaTiO_{3-\delta}$ are broad and the main peak P_F is visible only at the highest doping, make challenging an analysis like that carried out for $SrTiO_{3-\delta}$. In that case, it was possible to include in the analysis the temperature dependence of the populations of free and aggregated V_O, and the binding energies were estimated as $E_P = 0.18$ eV for pairs and 0.26 eV within longer chains[10]. The fits of the $BaTiO_{3-\delta}$ were instead carried out with expressions like Eq. (2), with temperature independent Δ, and in order to estimate the fraction of paired V_O, it was assumed that the V_O pair binding energy in $BaTiO_3$ has a value of ~ 0.2 eV, similar to $SrTiO_3$.

The $Q^{-1}(T)$ curves of BCTZ (Fig. 6) at increasing O deficiency are qualitatively similar to those of $BaTiO_{3-\delta}$ (Fig. 2), with the two major peaks P_P and P_F in the paraelectric phase, that shift to lower temperature with increasing δ, but these peaks are much broader and have larger activation energies. The broadening, quantified by the definitely smaller values of α and β in Table I, is justified by the disorder in the cation sizes, and renders difficult the analysis of the anelastic spectra. Therefore, the parameters of P_F for BCTZ in Table I are only indicative, and the fact that their activation energies are not slightly smaller at larger δ, as in $BaTiO_{3-\delta}$, should not be considered as significant.

Table I contains also the mean characteristic time τ for the hopping of an isolated V_O and reorientation of a V_O pair calculated at room temperature, useful for understanding the mechanisms of aging, fatigue and deterioration of properties. These times are only indicative, because neglect the splitting of the energies of the V_O with dipole parallel and perpendicular to the tetragonal axis in the FE phase, as explained later (Fig. 12). Some points can however be established: at room temperature the isolated V_O remain quite mobile, with hopping rates of about $1-10\ s^{-1}$ in all compositions. The reorientations of the pairs, and even more their dissociations, are slower, but still occur over time scales of minutes, except for BCTZ, which stands out with characteristic times of hundreds of years.

Considering the differences in the mobilities of free and aggregated V_O, it is important to know their relative fractions as a function of temperature. As already mentioned, the anelastic spectra of $BaTiO_3$ and BCTZ do not allow the binding energies of V_O in pairs and chains to be estimated, as it was done in $SrTiO_3$[10]. Yet, in order to have an idea, in Fig. 10, the relative fractions of isolated V_O at two representative total concentrations, $\delta = 0.003$ and 0.015, are plotted against T using the same method for analyzing the anelastic spectra of $SrTiO_{3-\delta}$. In one case, the same parameters of $SrTiO_3$ have been used, which should be representative of $BaTiO_3$, while the other case should represent BCTZ. Lacking estimates of the pair and chain binding energies for BCTZ, it has been taken into account that the activation energy for the pair reorientation in BCTZ, $W_P = 1.4$ eV, is 0.4 eV higher than in $SrTiO_3$ and 0.55 eV higher than in $BaTiO_3$, while W_F is higher by < 0.2 eV. This suggests that the pair binding energy of BCTZ is $0.2-0.3$ eV larger than in $SrTiO_3$ and $BaTiO_3$, namely $0.38-0.48$ eV. The curves in Fig. 10 are plotted using $E_P = E_C = 0.38$ eV, and indicate that, while in $BaTiO_{3-\delta}$ there is a sizeable fraction of free V_O around T_C and at RT, in BCTZ practically all V_O are aggregated and therefore static. This explains why BCTZ does not display any time dependence of T_C (Fig. 8).

2. *Pinning of domain walls by O vacancies*

Pinning of DW, at least of the 90° type, is demonstrated by the decrease of the dissipation below T_C by $5-10$ times upon introduction of as little as $\delta \sim 0.003$ V_O (Fig. 2). This dissipation is due to the relaxational motion of 90° DWs, which enlarge the fraction of the domains with *c* axis parallel to the extensional component of the sample vibration strain at the expenses of those perpendicular to it. There must be a broad distribution of characteristic times τ for the DW motion, resulting from the distribution of domain sizes and configurations, so that, rather than a peak centred at the temperature where $\omega\tau \sim 1$, the Q^{-1} curve is flat below T_C. It can be concluded that a considerable fraction of 90° DWs are pinned already by few tenths of percent of V_O. Nothing can be said about pinning of the 180° DWs, since their motion does not affect strain and does not contribute to the elastic energy dissipation. Notice, however, that the motion of any type of DW is also hindered by sparse quasistatic V_O by the fact that, while the DW sweeps through them, they temporarily transform from apical with lower energy to equatorial with higher energy (see Sect. IV E), effectively acting as a restoring force[26].

B. Dependence of T_C on history

The observation of a time dependence of T_C in ferroelectrics containing defects is not new. Enhancements of T_C up to 2.5 K have been observed in single crystals of $BaTiO_3$ after aging at RT for days[27], and attributed to the reorientation of $Fe'_{Ti}-V_O^{\cdot\cdot}$ electric dipoles parallel to the local spontaneous polarization. The corresponding lowering of the electric energy would stabilize the ferroelectric domains and enhance T_C[27]. A related effect is the shift and constriction of the hysteresis loops, due to the internal field created by the defect dipoles, preferentially aligned parallel to the local polar direction during aging[28,29].

Accordingly, the initial slow rise of T_C with aging over hours and days in the FE state of O deficient BT and BST (Figs. 3b,c and 5b) might be partly explained by a stabilization of the FE domains through the alignment of the orientations of the defect dipoles with respect to the local polarization, and stabilization of the DW configurations. In the present situations, the great majority of the V_O are introduced by the reduction treatments and are not paired with acceptor defects to form electric dipoles, but still the interaction of their elastic, instead of electric, dipoles with the tetragonal strain can

produce the same effect.

C. Apical and equatorial V_O in polar domains

In the FE tetragonal phase of a perovskite the O atoms become of two types: apical or equatorial with respect to the tetragonal c axis, as shown in Fig. 11, and differ in energy by $\Delta E_{ea} = E_e - E_a$, resulting in an interaction with the polar domain.

From a purely elastic point of view it should be $\Delta E_{ea} > 0$, assuming that the major axis of the V_O strain ellipsoid λ is parallel to the directions of the nearest neighbor Ti^{4+} ions, pushed away by the positive V_O, and in accordance with calculations[30]. The elastic contribution to ΔE_{ea} can be estimated as the energy difference of an elastic dipole between orientations parallel or perpendicular to the tetragonal strain. The anisotropic component of the elastic dipole of a V_O in cubic $BaTiO_3$, $\Delta\lambda = 0.077$, has been deduced from the intensity of peak P_F[18] and is very close to the calculated value of $\Delta\lambda = 0.067$[30]. The elastic contribution to the energy splitting between the two orientations in a tetragonal lattice can be written as[22]

$$\Delta E_{ea}^{elas} = v_0 \Delta\lambda \, (c_{33} - c_{13}) \, \varepsilon_T = 0.063 \text{ eV},$$

where $v_0 = 64.5 \times 10^{-30}$ m^3 is the cell volume, $c_{11} = 211$ GPa and $c_{13} = 107$ GPa the elastic constants and $\varepsilon_T = \frac{c}{a} = 0.01$ the tetragonal strain of $BaTiO_3$. This value is not far from $\Delta E_{ea} = 0.1$ eV, calculated for a V_O trapped by a Mn_{Ti}[31], and which takes into account also electronic effects and other differences between the actual FE lattice and a tetragonally strained PE lattice. Most of the calculations of the difference between the energies of the apical and equatorial sites for isolated V_O, including electronic effects, have been done for $PbTiO_3$, obtaining quite a broad range of results: $\Delta E_{ea} =$ 0.44 eV[26], 0.1 eV[32], 0.04 eV[33], 0.025 eV[34], -0.1 eV[35], -0.23 eV[36]. In the last paper ΔE_{ea} is also calculated for $BaTiO_3$ and found to be -0.06 eV, four times smaller than in $PbTiO_3$[36]. It is indeed expected that the magnitude of the splitting between the energies of V_O with elastic dipole parallel and perpendicular to the c axis is smaller in $BaTiO_3$ with $\frac{c}{a} = 0.01$ than in $PbTiO_3$ with $\frac{c}{a} = 0.065$.

Summing up, from a purely elastic point of view, the energy of a V_O in apical position should be $\Delta E_{ea}^{elas} \sim 0.063$ eV lower than in equatorial position. Taking into account first–principle calculations, which include the electronic effects, we may assume that $\Delta E_{ea} \gtrapprox 0.1$ eV. This has consequences with respect to the state and mobility of the V_O at RT, in the FE state: according to the Boltzmann factor $\exp(-\Delta E_{ea}/k_B T)$, only $\lessapprox 1/50$ of equatorial sites are occupied by V_O, implying almost total alignment of the elastic dipoles to the tetragonal axis at equilibrium, and the hopping rates between the two types of positions split by a factor of the same order of magnitude. These quantities cannot be measured by anelastic relaxation, because the relaxation spectrum below T_C is dominated by the DW relaxation.

The situation is illustrated in Fig. 12, with an Arrhenius plot of the relaxation times of peaks P_F and P_P in BT and BCTZ (green region) extrapolated in the FE state. It is assumed that the splitting of the activation energies in the FE phase is $\Delta E_{ea} = 0.1$ eV. The shaded region is the mean pair dissociation time assuming an activation energy up to 0.1 eV larger than that for reorientation (see the discussion of Fig. 9).

D. Dependence of electron doping and T_C on the aggregation of V_O

Having established that the V_O lack electric dipoles, but can influence the FE state through their elastic dipoles, we still observe that the magnitude of the changes of T_C with various temperature protocols in O deficient BT, and especially BST, are much larger than reported up to now in BT containing dopants or defects (see Sect. IV B). For example, in a single crystal of $BaTiO_3$ with unknown amount of Fe^{3+}–V_O complexes, T_C increased of up to 2.5 K after aging[27]; in $BaTiO_3$ doped with 1% Mn^{3+} on the Ti^{4+} site, and presumably $0.5 - 1\%$ compensating V_O, the shift was 1.5 K[37]. Evidently, in the presence of uncompensated V_O there must be another mechanism affecting T_C, besides the internal fields from the oriented defect dipoles. We are going to argue that the major factor affecting T_C is the electron doping from the ionized V_O, which depends on their aggregation state.

Let us first observe that the major cause of depression of T_C by doping is not the size effect of the dopants and defects, but the mobile charges that they induce. This is reasonable, if one considers that the mobile charges screen the dipolar interactions that induce ferroelectricity, and is demonstrated by the fact that uncompensated V_O depress T_C at a rate of about -4000 K/δ[18], but when they are electrically compensated as Schottky defects[38], the rate reduces to -220 K/δ in $Ba_{1-\delta}TiO_{3-\delta}$ and -820 K/δ in $BaTi_{1-\delta}O_{3-2\delta}$, inclusive of the contribution from the dopants. Accordingly, a neutral defect like Sr in $Ba_{1-x}Sr_xTiO_3$ reduces T_C by only -300 K/x[39]. Therefore, considering that the depression of T_C by charged defects is an order of magnitude larger than that by neutral defects, it is important to understand what effect the pairing and further aggregation of V_O has on the electron doping and finally on T_C.

We will not review the computational studies on the valence state of V_O and polarons from ionized V_O in $BaTiO_3$, because there is experimental evidence confirming the existence of V_O pairs and chains, independent of anelastic relaxation[10,18], and which also sheds light on the how these clusters affect doping. In fact, highly reduced films of $SrTiO_{3-\delta}$ have been studied by diffuse X-ray scattering, finding evidence of linear clusters along the [001] direction[11]. Moreover, photoemission spectroscopy revealed the presence of Ti^{2+}, in addition to Ti^{3+} and Ti^{4+}[11]. The [001] linear clusters are the V_O pairs and chains along the O–Ti–O directions, parallel to the polarization in the FE state and the Ti^{2+} ions are within such pairs and chains[11]. The Ti^{3+} correspond to the mobile electrons in band

or polaron states, responsible for the nearly metallic conductivity of the reduced samples, while the two electrons at the Ti^{2+} sites are evidently localized.

The emerging picture is that isolated V_O are doubly charged and dope two electrons each, but, if two V_O form a pair, doping is halved, because two electrons are localized on the intermediate Ti^{2+}. Further aggregation of V_O to form longer chains creates new Ti^{2+} ions and halves the doping. Therefore, *full pairing/clustering of the V_O halves the electron doping, with respect to the case of fully dispersed V_O*.

As explained in Sect. IV A 1, it is difficult to be quantitative on the fraction of aggregated V_O during temperature runs and aging for predicting the consequences on T_C, but we may use Fig. 10 as a guide. In addition to the uncertainties on the binding energies, one should take into account the slow rate for reaching equilibrium, as mentioned in Sect. IV A 1. In fact, the high mobility of the free V_O (~ 10 jump/s at RT according to Table I) would suggest that the equilibrium fraction of aggregated V_O is reached almost instantaneously above RT and T_C, but in fact the rate for aggregation is slower than that for free hopping, due to the electrostatic repulsion, which raises the saddle point for joining another V_O (Fig. 9). The rise estimated for $SrTiO_3$, $\Delta W_{el} = 0.19$ eV, causes a slowing of the aggregation the rate by 250 times at 400 K and 2500 times at RT. In addition, if V_O chains have lower energy than pairs, as in $SrTiO_3$, the conversion of sparse pairs into chains requires the dissociation of some of them, which is slower than the pair reorientation rate (according to Fig. 12 as slow as 1 jump/hour at RT). The slow kinetics for reaching the thermal equilibrium between isolated and aggregated V_O may account for the fact that it is not sufficient to enter the PE phase in order to reach a stable state, and both the $Q^{-1}(T)$ and $E(T)$ curves, including T_C, are not always reproducible also during cooling.

Since the V_O aggregation decreases doping and enhances T_C, the slow kinetics for aggregation, may be the major cause of the increase of T_C with aging in the FE state, and adds to the known stabilization effects of the FE domains. An indication in this sense comes from the comparison of heating and subsequent cooling after long aging in Fig. 4b. During heating, peak P_F due to the hopping of free V_O is more intense, indicating a higher fraction of free V_O and hence higher doping, and T_C is indeed lower. In addition, P_F is also shifted to lower temperature, coherent with higher doping. During cooling the opposite is observed in peak P_F and T_C, coherent with a reduced amount of V_O and doping than previously. These phenomena are amplified by mild lattice disorder, as in BST with 3% Sr (Fig. 5), presumably due to the distribution of hopping rates with tails of longer relaxation times.

Explaining the details of the approach to equilibrium during the temperature runs or short aging times seems an exceedingly difficult task, but we would now try to explain the puzzling observation that, after an extremely long aging (6 years in Fig. 4a), T_C does not actually further increase and saturate, but becomes smaller. In order to do that, we should consider the competition between the clustering of V_O into V_O–Ti–V_O pairs and chains along the [001] direction and their association to the DWs.

E. Pinning of 90° domain walls by isolated V_O and increase of electron doping.

As noted in Sect. IV A 2, the marked depression of Q^{-1} below T_C after the introduction of V_O, proves that the DW are pinned by V_O. Yet, this does not necessarily imply that the aggregation state of V_O is affected by DWs. It would be possible that the direct DW–V_O interaction is weak, the V_O remain within the domains, and pinning is due to the effective restoring force acting when the DW sweeps through them, and they temporarily transform from apical with lower energy to equatorial with higher energy[26].

In order to establish whether the interaction between V_O and DW may affect the aggregation state of V_O, it is necessary to compare the respective binding energies and consider in detail which positions would the V_O occupy with respect to the DW. To this end, we will review the relevant literature on the nature of the interaction between V_O and DWs in perovskite ferroelectrics.

In the FE-T phase, the DWs can separate domains whose spontaneous polarizations are rotated by 180° and 90°, which in turn can be neutral head-to-tail DWs or charged head–to–head or tail–to–tail[40]. Negatively charged tail–to–tail DWs are the most effective traps for positively charged $V_O^{\cdot\cdot}$, but charged DWs are energetically unfavorable and therefore rare, unless specific poling procedures are used[41]. This is not the case of our unpoled samples and we will assume that the DWs are neutral 90° and 180°. On the other hand, it has been proposed that V_O may nucleate tail–to–tail DWs and distribute along them[42], so that we cannot exclude that, especially at the highest O deficiencies, also charged tail–to–tail DW decorated with V_O exist. Even neutral 90° DW, however, have a local electric field, due to the change of direction of the spontaneous polarization. This field is absent in 180° DW and accumulates positively charged defects and electrons on either sides of the wall[43], so that, in general, there is stronger attraction between V_O and 90° DWs.

Coming to $BaTiO_3$, in most of the experimental studies on pinning of DWs, the V_O electrically compensate acceptors, like Mn^{3+} or Fe^{3+} substituting Ti^{4+}, intentionally doped or as unwanted impurities. Since V_O are strongly bound to the acceptors, which are static, those results are not indicative of DW pinning from mobile V_O.

First–principle calculations of V_O at both 180° an 90° DWs have been done mainly for $PbTiO_3$. The 180° DW is found to be extremely sharp, only one unit cell in both directions, and the energy of a doubly charged $V_O^{\cdot\cdot}$ at the DW is 0.13 eV lower than far from it[44], in substantial agreement with a previous study[45]. In the case of 90° DW in $PbTiO_3$, it has been found that both apical and equatorial V_O lower their energy of $\sim$ 0.2 eV[26] or 0.23–0.33 eV[34,35] within the DW or in positions nearest neighbor to it. The first–principle calculations indicate that the sites of lowest energy for the V_O are on the tail side of 90° DW, contrary to what suggested by more macroscopic phase–field calculation schemes[43].

Similar calculations for $BaTiO_3$ are not available, except for 180° DW, where it is found that, at variance with $PbTiO_3$, V_O in $BaTiO_3$ have lower energy within the domains than near

180° DW, and concluding that DW pinning by V_O should be either weak or entirely absent in $BaTiO_3$[46]. This is neither in contradiction nor in agreement with our data, since we are not sensitive to the motion of 180° DW. Moreover, considering that 180° DWs have a higher formation energy than 90° DWs (>4 times in $PbTiO_3$[35]), and lack their internal electric fields[43], the weakness or absence of interaction of V_O with 180° DW seems irrelevant to our discussion.

Considering that the tetragonal strain and internal electric fields in $BaTiO_3$ are smaller than in $PbTiO_3$, we may take the magnitude of the binding energies between a V_O and a 90° DW in $PbTiO_3$, up to 0.33 eV, as an upper limit for $BaTiO_3$. Therefore, it appears that the magnitude of the binding energy to the 90° DW is competitive with the V_O pair binding energy $E_P \simeq 0.18$ eV in $SrTiO_3$[10], which we assume is similar, if not smaller, in $BaTiO_3$[18].

It is therefore possible that after a long equilibration time the V_O pairs split and migrate to 90° DWs, where the most favorable configuration is no more that of stable V_O–Ti–V_O pairs and chains. This is evident in Fig. 13a, showing a domain ending at the bottom in a 90° DW, with the TiO_6 octahedra put in evidence. The O atoms are distinguished into apical and equatorial. We have seen that the Boltzmann factor $\exp(-\Delta E_{ea}/k_B T)$ at RT makes an apical V_O tens of times more favorable than an equatorial one, both far and near a DW. Therefore, the V_O occupy only the apical positions, both when they are isolated and aggregated, and the stable V_O pairs and chains in the FE state are along these [001] O–Ti–O rows, but it is clear that no such pair can have both V_O at the DW plane. In fact, if a pair is along the c direction, within the horizontal plane of Fig. 13a, then only one of the two V_O is at the DW, and the DFT calculations show very sharp differences between the optimal position at the DW and away from it[34,35]. Neither can any pair of sites in the plane of the DW form a stable pair of V_O at opposite sides of a same Ti atom, since different apical O sites belong to different octahedra.

Figure 13b shows what happens when a stable pair of V_O, sharing a Ti^{2+} ion, dissociates in order to have both V_O at the DW: the number of mobile Ti^{3+} electrons doubles from 2 to 4, as explained in Sect. IV D.

In the light of the above considerations, we propose the following explanation for the fact that T_C increases with aging on the time scale of days but then decreases after years (Fig. 4a). When cooling from the PE state through T_C, about half of the V_O are free (Fig. 10) and, in addition to continuing to aggregate, they can quickly pin the forming DWs, as demonstrated by the fact that the elastic energy loss of the O deficient samples is depressed immediately below T_C, with respect to the case $\delta = 0$. The first stage of aging at RT would see a clamping of the DWs mainly by free V_O, which does not change doping, and an increase of the aggregated fraction far from the DWs, according to Fig. 10, which decreases doping and raises T_C. Yet, if the V_O are slightly more stable at the DWs than in pairs and chains, which seems to be the case, on a long time scale, part of the already aggregated V_O will dissociate and migrate to the DWs, accounting for the final decrease of T_C. The relaxation times extrapolated at RT in Fig. 12, together with the equilibrium fractions of isolated and aggregated V_O in Fig. 10, justify the observation of the rich phenomenology found in the aging dependence of T_C in BT and BST.

F. Absence of aging in BCTZ

Figure 8 demonstrates that, contrary to BT and BST, aging has no effect on T_C in BCTZ. This is again explained by the combination of Figs. 10 and 12: at RT practically all V_O are aggregated and their mean dissociation rate is of the order of hundreds of years. This may also provide a justification to the better resistance to bipolar fatigue[47] and absence of pinched P-E loops starting from the unpoled state found in BCTZ[48].

V. CONCLUSIONS

The Young's modulus and elastic energy loss, Q^{-1}, of $BaTiO_{3-\delta}$, $Ba_xSr_{1-x}TiO_{3-\delta}$ and $(Ba_{0.85}Ca_{0.15})(Zr_{0.1}Ti_{0.9})O_{3-\delta}$ have been repeatedly measured during heating and cooling runs at various O deficiencies and after different aging times. The $Q^{-1}(T)$ curves in the paraelectric phase contain peaks due to the isolated and paired V_O, from which it is possible to measure the respective hopping/reorientation rates and activation energies, while in the ferroelectric phase they monitor the degree of domain wall pinning by V_O.

The V_O are introduced by reducing treatments and are free to diffuse and aggregate into pairs, while in most applications they are compensating acceptor dopants, with which form complexes stable at room temperature. A major consequence is that the dependence of T_C and its thermal hysteresis on aging and history are greatly enhanced: in BT (BST) we found that T_C measured during heating may vary of 6 K (21 K) at the same value of δ, while no anomaly is found in BCTZ. The main conclusions are that T_C is depressed mainly by the mobile electrons doped by V_O. Each isolated V_O dopes two mobile electrons as Ti^{3+} ions, but, when it forms a stable linear V_O–Ti^{2+}–V_O pair, the two electrons of the Ti^{2+} ion are immobile and do not contribute to doping. Therefore, T_C is determined not only by the O deficiency δ but also by the fraction of V_O that are aggregated. In this manner it is possible to explain the rise of T_C during initial aging, much larger than in acceptor doped $BaTiO_3$, where the V_O remain bound to the acceptor and do not change the doping level.

While a mild lattice disorder (up to 10% Sr substituting Ba) increases the effects, the strong disorder of BCTZ completely freezes them. In fact, BCTZ has a much larger mean activation energy for the pair reorientation (1.4 eV compared to ≤ 0.86 eV in BT) and hence for the pair dissociation. At room temperature practically all V_O are paired and static over a time scale of hundred years, explaining the superior resistance of BCTZ to fatigue[47].

In order to explain the fact that during long aging (here 6 years) T_C does not continue increasing and saturate, but actually decreases, the interaction between V_O and 90° DW has

been considered in detail. It is shown that the stable linear V_O–Ti–V_O pairs along the polarization direction cannot optimize their position with respect to the DW plane. Therefore, over a long time scale, the V_O initially in stable pairs within the domains, migrate and dissociate in order to decorate the 90° DW, increasing doping and lowering T_C.

Acknowledgments

This work has been partially funded by the PRIN SELWA Project, Next Generation EU n. 20229PNWM7 and the São Paulo Research Foundation FAPESP, Brazil (Grant No. 2022/08030-5). FC and FC acknowledge the precious technical assistance of M.P. Latino (CNR-ISM).

* Electronic address: francesco.cordero@ism.cnr.it
† Electronic address: elisa.mercadelli@issmc.cnr.it

[1] Y. A. Genenko, J. Glaum, M. J. Hoffmann, and K. Albe, *"Mechanisms of aging and fatigue in ferroelectrics,"* Mater. Sci. Engin. B **192**, 52 (2015).
[2] M. Tyunina, *"Oxygen Vacancies in Perovskite Oxide Piezoelectrics,"* Materials **13**, 5596 (2020).
[3] J. Chun, J. Heo, K. Lee, B. U. Ye, and B. S. K. S.-H. Yoon, *"Thermal activation energy on electrical degradation process in $BaTiO_3$ based multilayer ceramic capacitors for lifetime reliability,"* Sci. Rep. **14**, 616 (2024).
[4] M. R. Opitz, K. Albertsen, J. J. Beeson, D. F. Hennings, J. L. Routbort, and C. A. Randall, *"Kinetic Process of Reoxidation of Base Metal Technology $BaTiO_3$-Based Multilayer Capacitors,"* J. Am. Ceram. Soc. **86**, 1879 (2003).
[5] F. Zhang, J. Tan, P. Wang, R. Huang, H.-T. Lin, X. Huang, J. Yang, Z. Fu, X. Cao, L. Zhang, S. Yu, and R. Sun, *"Defect dipole engineering enhanced the dielectric performance and reliability of Mn-doped $BaTiO_3$-based multilayer ceramic capacitor,"* Ceram. Int. **50**, 38263 (2024).
[6] G. Huangfu, J. Wang, H. Zhang, J. Chen, Z. Liu, and Y. Guo, *"Deciphering the Effect of Defect Dipoles on the Polarization and Electrostrain Behavior in Perovskite Ferroelectrics,"* Nano Lett. **24**, 12148 (2024).
[7] H. Zheng, E. Sun, X. Qi, B. Yang, R. Zhang, and W. Cao, *"Temperature and frequency dependent defect dipole kinematics in "hard" piezoelectric ceramics,"* Sens. Actuators A: Phys. **344**, 113712 (2022).
[8] R. A. D. Souza, *"Oxygen Diffusion in $SrTiO_3$ and Related Perovskite Oxides,"* Adv. Func. Mater. **25**, 6326 (2015).
[9] N. H. Chan, R. K. Sharma, and D. M. Smyth, *"Nonstoichiometry in undoped $BaTiO_3$,"* J. Am. Ceram. Soc. **64**, 556 (1981).
[10] F. Cordero, *"Hopping and clustering of oxygen vacancies in $SrTiO_3$ by anelastic relaxation,"* Phys. Rev. B **76**, 172106 (2007).
[11] K. Eom, E. Choi, M. Choi, S. Han, H. Zhou, and J. Lee, *"Oxygen Vacancy Linear Clustering in a Perovskite Oxide,"* J. Phys. Chem. Lett. **8**, 3500 (2017).
[12] A. Hackmann and O. Kanert, *"NMR investigation of defect properties in single crystal $SrTiO_3$,"* Radiation Effects and Defects in Solids **119**, 651 (1991).
[13] A. Buzlukov, A. Trokiner, V. Kozhevnikov, S. Verkhovskii, A. Yakubovsky, I. Leonidov, A. Gerashenko, A. Stepanov, and I. B. A. Tankeyev, *"Vacancy ordering and oxygen dynamics in oxide ion conducting $La_{1-x}Sr_xGa_{1-x}MgxO_{3-x}$ ceramics: ^{71}Ga, ^{25}Mg and ^{17}O NMR,"* J. Solid State Chem. **184**, 36 (2011).
[14] R. A. Eichel, *"Defect structure of oxide ferroelectrics-valence state, site of incorporation, mechanisms of charge compensation and internal bias fields,"* J. Electroceram. **19**, 9 (2007).
[15] M. Tyunina and M. Savinov, *"Charge transport in epitaxial barium titanate films,"* Phys. Rev. B **101**, 094106 (2020).
[16] G. Y. Yang, E. C. Dickey, C. A. Randall, M. S. Randall, and L. A. Mann, *"Modulated and ordered defect structures in electrically degraded Ni-$BaTiO_3$ multilayer ceramic capacitors,"* J. Appl. Phys. **94**, 5990 (2003).
[17] F. Cordero, F. Trequattrini, F. Craciun, H. T. Langhammer, D. A. B. Quiroga, and J. P. S. Silva, *"Probing ferroelectricity in highly conducting materials through their elastic response: Persistence of ferroelectricity in metallic $BaTiO_{3-\delta}$,"* Phys. Rev. B **99**, 064106 (2019).
[18] F. Cordero, F. Trequattrini, D. A. B. Quiroga, and P. S. S. Jr., *"Hopping and clustering of oxygen vacancies in $BaTiO_{3-\delta}$ and the influence of the off-centred Ti atoms,"* J. Alloys Compd. **874**, 159753 (2021).
[19] F. Cordero, F. Trequattrini, P. S. da Silva, Jr., M. Venet, O. Aktas, and E. K. H. Salje, *"Elastic precursor effects during $Ba_{1-x}Sr_xTiO_3$ ferroelastic phase transitions,"* Phys. Rev. Research **5**, 013121 (2023).
[20] P. Wang, L. Zhang, S. Yu, R. Sun, Z. Fu, and X. Cao, in *24th International Conference on Electronic Packaging Technology (ICEPT)* (IEEE, 2023).
[21] F. Cordero, L. Dalla Bella, F. Corvasce, P. M. Latino, and A. Morbidini, *"An insert for anelastic spectroscopy measurements from 80 K to 1100 K,"* Meas. Sci. Technol. **20**, 015702 (2009).
[22] A. S. Nowick and B. S. Berry, *Anelastic Relaxation in Crystalline Solids* (Academic Press, New York, 1972).
[23] F. Cordero, *"Anelastic (dielectric) relaxation of point defects at any concentration, with blocking effects and formation of complexes,"* Phys. Rev. B **47**, 7674 (1993).
[24] G. Cannelli, R. Cantelli, F. Cordero, N. Piraccini, F. Trequattrini, and M. Ferretti, *"Mobility and aggregation of oxygen in $YBa_2Cu_3O_{6+x}$ in the low- concentration limit,"* Phys. Rev. B **50**, 16679 (1994).
[25] F. Cordero, F. Craciun, and F. Trequattrini, *"Ionic Mobility and Phase Transitions in Perovskite Oxides for Energy Applications,"* Challenges **8**, 5 (2017).
[26] A. Chandrasekaran, X. K. Wei, L. Feigl, D. Damjanovic, N. Setter, and N. Marzari, *"Asymmetric structure of 90° domain walls and interactions with defects in $PbTiO_3$,"* Phys. Rev. B **93**, 144102 (2016).
[27] D. Sun, X. Ren, and K. Otsuka, *"Stabilization effect in ferroelectric materials during aging in ferroelectric state,"* Appl. Phys. Lett. **87**, 142903 (2005).

[28] K. Carl and K. H. Hardtl, *"Electrical after-effects in Pb(Ti, Zr)O_3ceramics,"* Ferroelectrics **17**, 473 (1977).

[29] X. Ren, *"Large electric-field-induced strain in ferroelectric crystals by point-defect-mediated reversible domain switching,"* Nat. Mater. **3**, 91 (2004).

[30] E. J. Granhed, A. Lindman, C. Eklöf-Österberg, M. Karlsson, S. F. Parker, and G. Wahnström, *"Band vs. polaron: vibrational motion and chemical expansion of hydride ions as signatures for the electronic character in oxyhydride barium titanate,"* J. Mater. Chem. A **7**, 16211 (2019).

[31] J. F. Nossa, I. I. Naumov, and R. E. Cohen, *"Effects of manganese addition on the electronic structure of $BaTiO_3$,"* Phys. Rev. B **91**, 214105 (2015).

[32] T. Shimada, T. Ueda, J. Wang, and T. Kitamura, *"Hybrid Hartree-Fock density functional study of charged point defects in ferroelectric $PbTiO_3$,"* Phys. Rev. B **87**, 174111 (2013).

[33] Y. Yao and H. Fu, *"Charged vacancies in ferroelectric $PbTiO_3$: Formation energies, optimal Fermi region, and influence on local polarization,"* Phys. Rev. B **84**, 064112 (2011).

[34] T. Xu, T. Shimada, Y. Araki, J. Wang, and T. Kitamura, *"Multiferroic Domain Walls in Ferroelectric $PbTiO_3$ with Oxygen Deficiency,"* Nano Lett. **16**, 454 (2016).

[35] X. Wang, T. Xu, F. Xuan, C. Chen, T. Shimada, and T. Kitamura, *"Effect of the oxygen vacancy on the ferroelectricity of 90° domain wall structure in $PbTiO_3$: A density functional theory study,"* J. Appl. Phys. **126**, 174107 (2019).

[36] Z. Alahmed and H. X. Fu, *"First-principles determination of chemical potentials and vacancy formation energies in $PbTiO_3$ and $BaTiO_3$,"* Phys. Rev. B **76**, 224101 (2007).

[37] M. M. Ahmad, K. Yamada, P. Meuffels, and R. Waser, *"Aging-induced dielectric relaxation in barium titanate ceramics,"* Appl. Phys. Lett. **90**, 112902 (2007).

[38] S. Lee, Z.-K. Liu, M.-H. Kim, and C. A. Randall, *"Influence of nonstoichiometry on ferroelectric phase transition in $BaTiO_3$,"* J. Appl. Phys. **101**, 054119 (2007).

[39] V. V. Lemanov, E. P. Smirnova, P. P. Syrnikov, and E. A. Tarakanov, *"Phase transitions and glasslike behavior in $Sr_{1-x}Ba_xTiO_3$,"* Phys. Rev. B **54**, 3151 (1996).

[40] P. Ondrejkovic, P. Marton, M. Guennou, N. Setter, and J. Hlinka, *"Piezoelectric properties of twinned ferroelectric perovskites with head-to-head and tail-to-tail domain walls,"* Phys. Rev. B **88**, 024114 (2013).

[41] T. Sluka, A. K. Tagantsev, D. Damjanovic, M. Gureev, and N. Setter, *"Enhanced electromechanical response of ferroelectrics due to charged domain walls,"* Nat. Commun. **4**, 1751 (2012).

[42] U. Petralanda, M. Kruse, H. Simons, and T. Olsen, *"Oxygen Vacancies Nucleate Charged Domain Walls in Ferroelectrics,"* Phys. Rev. Lett. **127**, 117601 (2021).

[43] L. Hong, A. K. Soh, Q. G. Du, and J. Y. Li, *"Interaction of o vacancies and domain structures in single crystal $BaTiO_3$: Two-dimensional ferroelectric model,"* Phys. Rev. B **77**, 094104 (2008).

[44] A. Chandrasekaran, D. Damjanovic, N. Setter, and N. Marzari, *"Defect ordering and defect-domain-wall interactions in $PbTiO_3$: A first-principles study,"* Phys. Rev. B **88**, 214116 (2013).

[45] L. He and D. Vanderbilt, *"First-principles study of oxygen-vacancy pinning of domain walls in $PbTiO_3$,"* Phys. Rev. B **68**, 134103 (2003).

[46] A. Samanta, S. Yadav, Z. Gu, C. G. Meyers, L. Wu, D. Chen, S. Pandya, R. A. York, L. W. Martin, J. E. Spanier, and I. Grinberg, *"A Predictive Theory for Domain Walls in Oxide Ferroelectrics Based on Interatomic Interactions and its Implications for Collective Material Properties,"* Adv. Mater. **34**, 2106021 (2021).

[47] Z. Fan, J. Koruza, J. Rödel, and X. Tan, *"An ideal amplitude window against electric fatigue in $BaTiO_3$-based lead-free piezoelectric materials,"* Acta Mater. **151**, 253 (2018).

[48] Y. Zhang, J. Glaum, M. C. Ehmke, K. J. Bowman, J. E. Blendell, and M. J. Hoffman, *"The ageing and de-ageing behaviour of $(Ba_{0.8}5Ca_{0.15})(Ti_{0.9}Zr_{0.1})O_3$ lead-free piezoelectric ceramics,"* J. Appl. Phys. **118**, 124108 (2015).

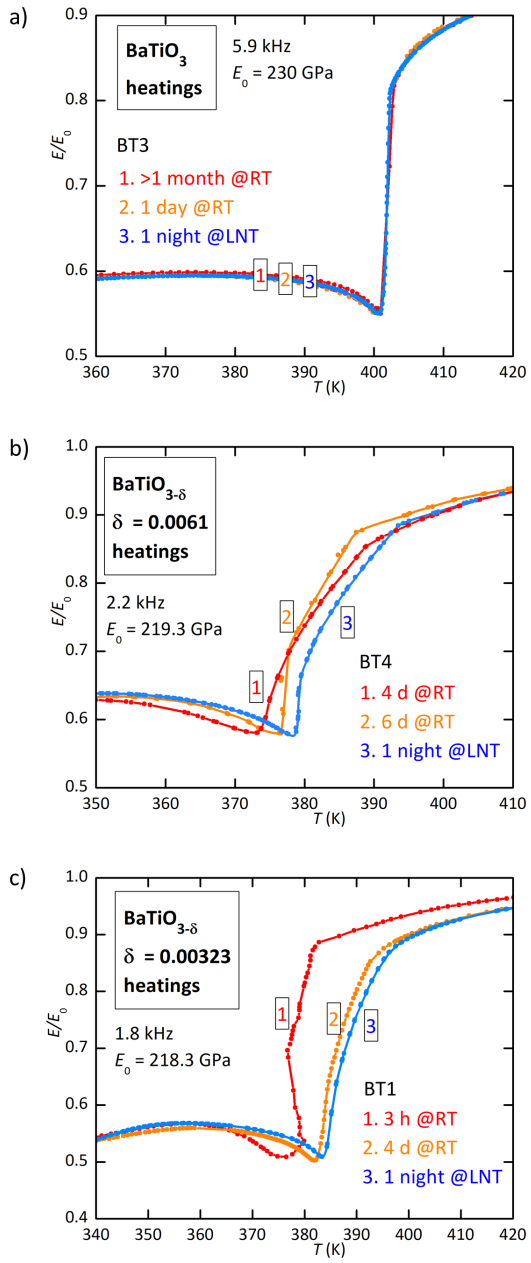

FIG. 3: Normalized Young's modulus of $BaTiO_{3-\delta}$ measured around T_C in various conditions. The legends indicate the aging times after high temperature treatments or measurements, that should have reset the state of the sample. a) sample BT3 with $\delta = 0$ after > 1 month (1) and 1 day (2) at room temperature (RT) and after one night at liquid N_2 temperature (LNT) (3). b) sample BT4 with $\delta = 0.0061$ after 4 days (1) and 6 days (2) at RT and after one night at LNT (3). c) sample BT1 with $\delta = 0.0032$ after 3 h (1) and 4 days (2) at RT and after one night at LNT (3); in curve (1) there was an inversion of the temperature rate through the transition.

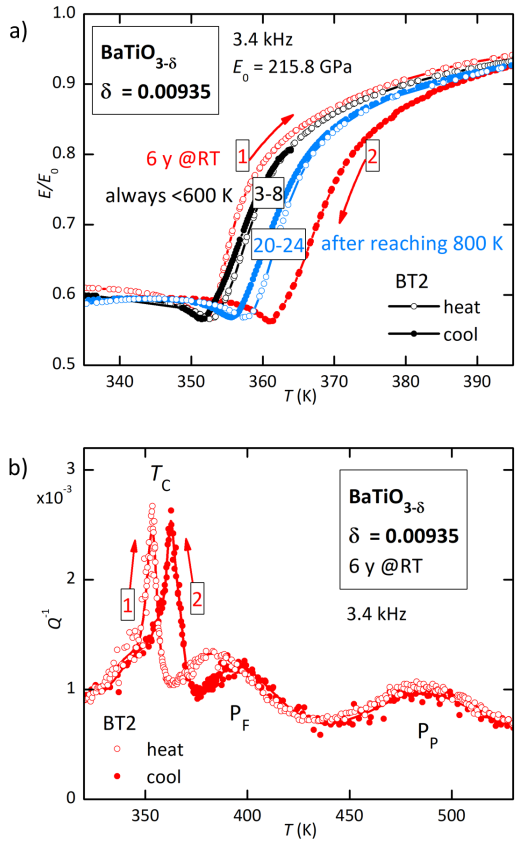

FIG. 4: a) Normalized Young's modulus of sample BT2 with $\delta = 0.00935$ measured during heating and cooling after 6 years aging at RT (1,2), subsequent cycles not exceeding 600 K (3-8), subsequent cycles after having reached 800 K (20-24). b) Q^{-1} measured together with the E of curves (1,2) in a).

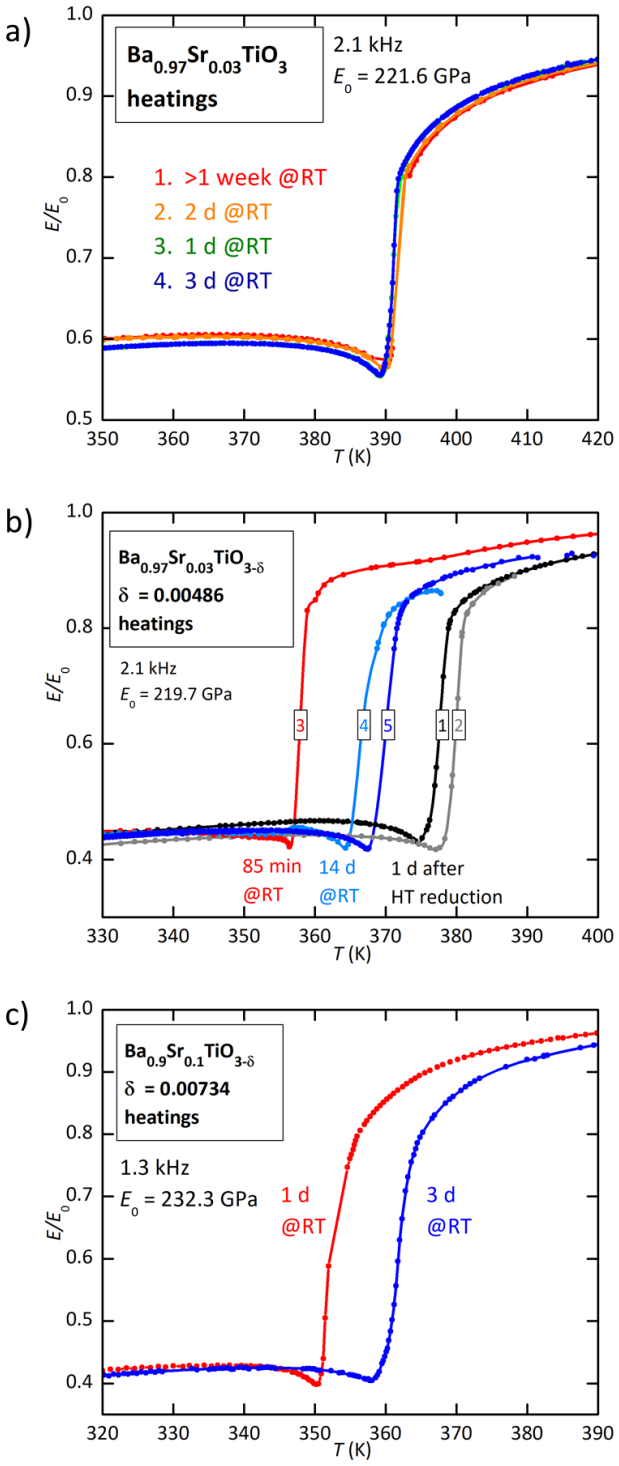

FIG. 5: Young's modulus of $Ba_{0.9}Sr_{0.1}TiO_{3-\delta}$ normalized to its maximum value measured during heating with: a) $\delta = 0$ after aging at RT for the times indicated in the figure; b) $\delta = 0.000486$, one day after the reduction treatment (1) repeated the following day (2) up to 390 K, immediately followed by a permanence of 1.5 h at RT (3); after 14 days at RT (4), immediately cooling past the transition e re-heating (5).

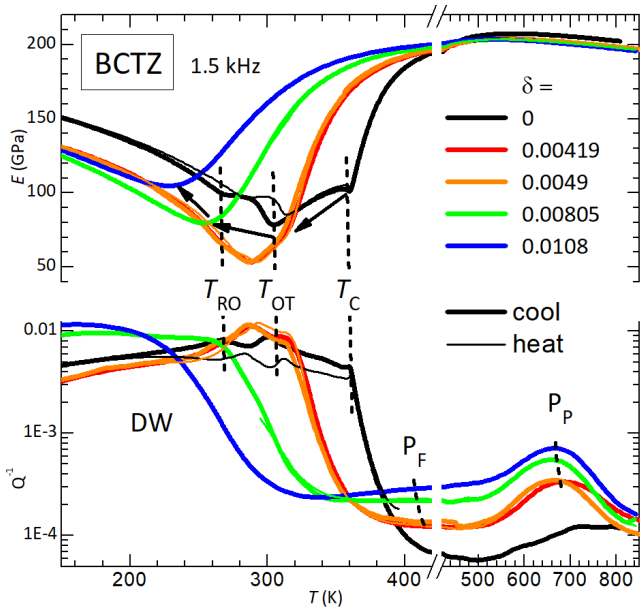

FIG. 6: Young's modulus E and elastic energy loss coefficient Q^{-1} of $(Ba_{0.85}Ca_{0.15})(Zr_{0.1}Ti_{0.9})O_{3-\delta}$ at various O deficiencies δ. The arrows indicate the shift of T_C with increasing δ. The thick lines are measured during cooling and the thin lines during heating; the difference between the two is noticeable only at the lowest O deficiencies in the region of the phase transitions.

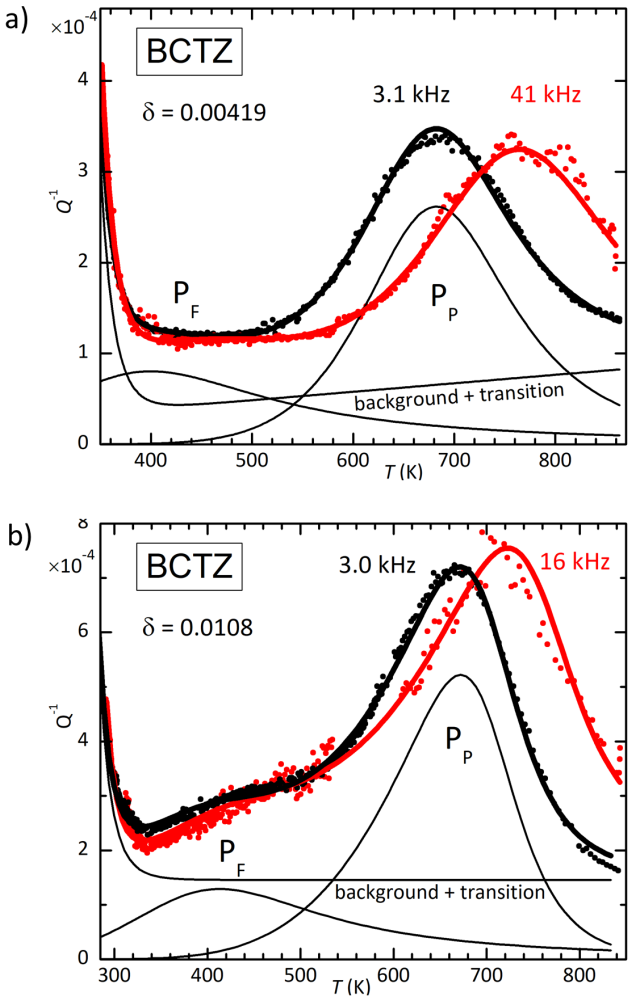

FIG. 7: The continuous lines are fits of the elastic energy loss coefficient Q^{-1}in the paraelectric phase of O deficient $(Ba_{0.85}Ca_{0.15})(Zr_{0.1}Ti_{0.9})O_{3-\delta}$. a) $\delta = 0.00419$ measured exciting the 1st and 5th modes; b) $\delta = 0.0108$ measured exciting the 1st and 3rd modes.

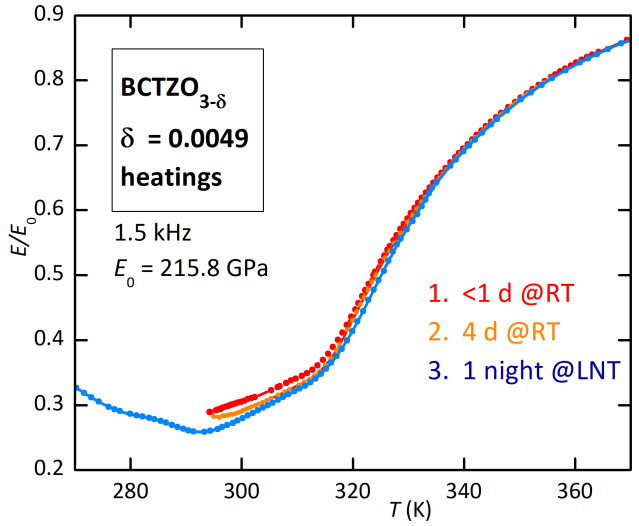

FIG. 8: Young's modulus E and elastic energy loss coefficient Q^{-1} of $(Ba_{0.85}Ca_{0.15})(Zr_{0.1}Ti_{0.9})O_{3-\delta}$ with $\delta = 0.0049$ after various agings in the FE state.

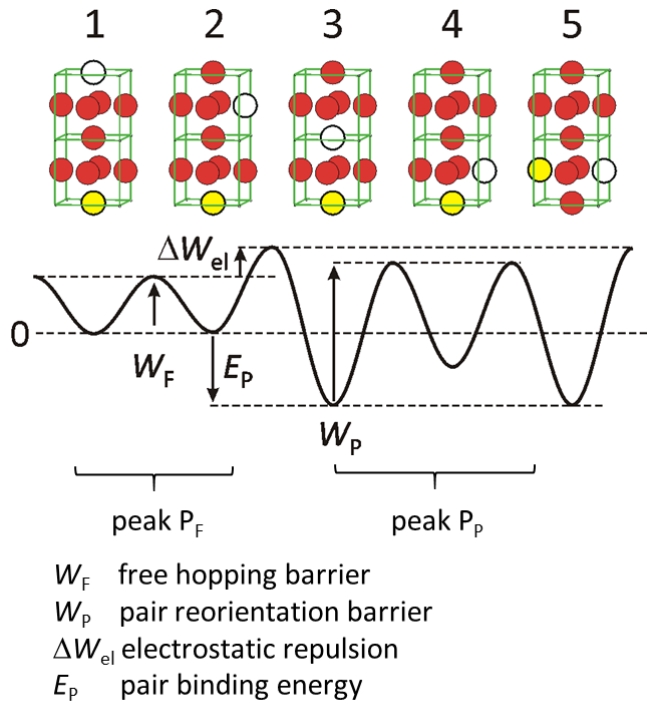

FIG. 9: Potential profile for passing from configuration 1 to 5, where the white V_O approaches the yellow one and forms a stable pair (3), which reorients (4,5).

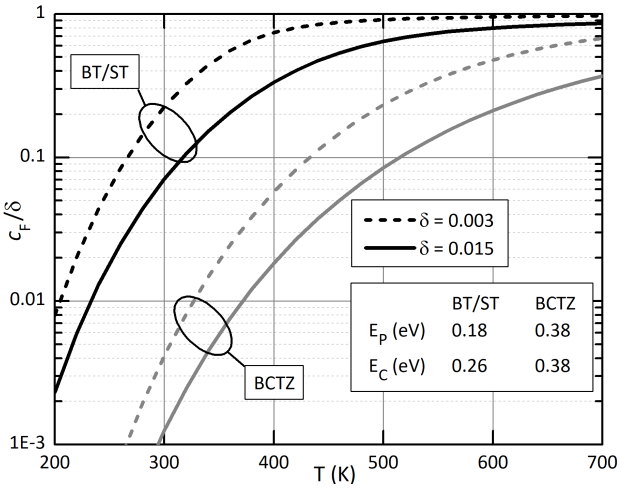

FIG. 10: Relative fractions of isolated V_O calculated with the method used for $SrTiO_{3-\delta}$[10] at two representative total concentrations $\delta = 0.003, 0.015$ using a) the same binding energies of $SrTiO_3$, supposed to be valid also for $BaTiO_3$; b) larger binding energies representative of BCTZ.

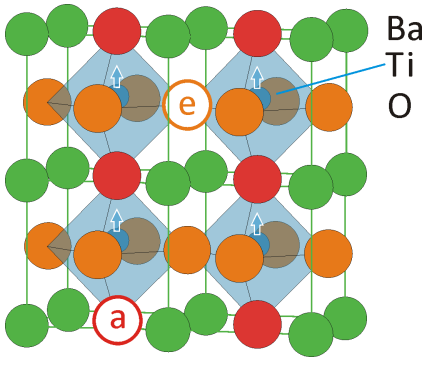

FIG. 11: Lattice of ferroelectric tetragonal $BaTiO_3$ with apical (red) and equatorial (orange) O^{2-} ions and two respective vacancies. The arrows are the polar displacements of the Ti atoms.

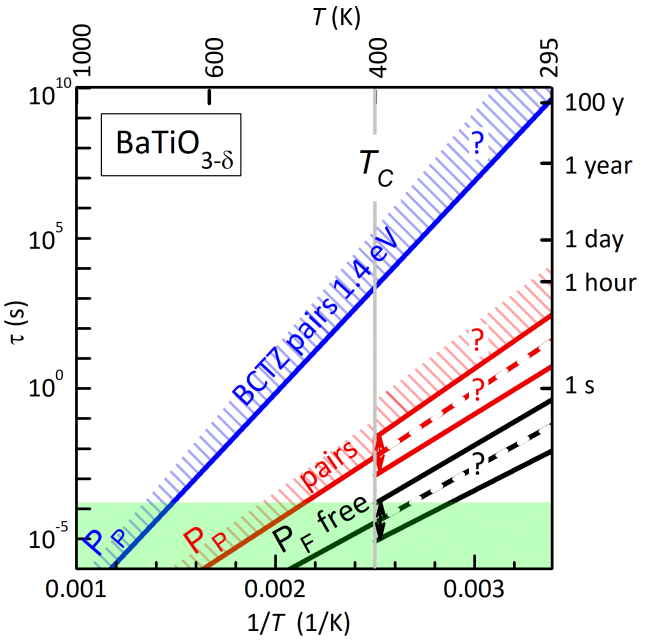

FIG. 12: Arrhenius plot of the relaxation times of peaks P_F and P_P in BT and BCTZ (green region) extrapolated in the FE state. It is assumed that the splitting of the activation energies in the FE phase is $\Delta E_{ea} = 0.1$ eV. The shaded region is the mean pair dissociation time assuming an activation energy up to 0.1 eV larger than that for reorientation.

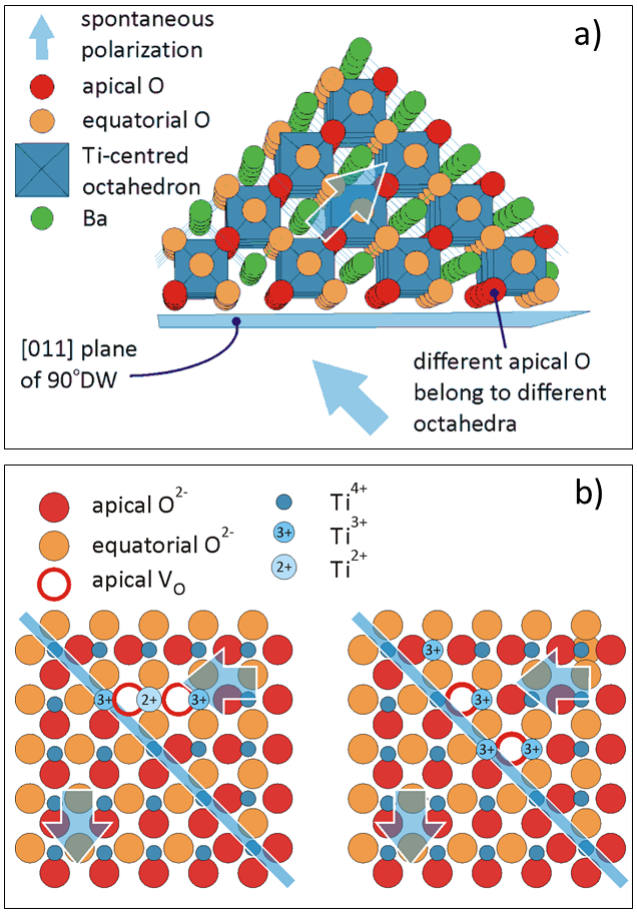

FIG. 13: a) 90° DW of $BaTiO_3$. All the apical O atoms in planes parallel to the DW belong to different octahedra. b) TiO_2 plane of $BaTiO_3$ with 90° DW (cyan line) and two V_O. The energy of V_O in the equatorial positions is higher than in the apical positions. On the left, an in-line V_O–Ti–V_O pair, where only one V_O has the energy lowered by the DW, contributes two mobile Ti^{3+} electrons. On the right, the pair is dissociated in order have both V_O in the lowest energy positions and contributes four mobile electrons.